International Forum on Aeroelasticity and Structural Dynamics
IFASD 2024
17-21 June 2024, The Hague, The Netherlands

ASSESSMENT OF THE AEROELASTIC STABILITY OF HIGH ASPECT RATIO WING AIRCRAFT DURING THE PRELIMINARY DESIGN

Sunpeth Cumnuantip[1*], Matthias Schulze [1], Wolf R. Krüger [1]

[1] DLR – Institute of Aeroelasticity, Bunsenstr. 10, 37073 Göttingen, Germany
[*]sunpeth.cumnuantip@dlr.de

Keywords: aeroelastic stability, high aspect ratio wing aircraft, preliminary design

Abstract: One concept to reduce an aircraft's fuel consumption is to increase the aspect ratio of the wing. Although such slender wings have low induced drag, a number of aeroelastic issues arise. As an example, high aspect ratio wings are relatively soft in bending and torsion when compared to conventional designs. These structural properties can lead to a reduction of the flutter speed. In the current research projects VirEnfREI and UP Wing, the Institute of Aeroelasticity of the German Aerospace Center performs the aeroelastic stability assessment of short/medium-range transport aircraft configurations equipped with high aspect ratio wings during the preliminary design phase. This paper compares results of preliminary aeroelastic stability assessments and discusses influences from the structural design on the aeroelastic behavior of the wings.

1 INTRODUCTION

A reduction of the aerodynamic drag is one of the possibilities to reduce the fuel consumption of an aircraft. The induced drag, being a major contributor to the total aerodynamic drag, can be reduced by increasing the wing aspect ratio, i. e. the relation between the wing span, wing area and wing chord. In the case of the same wing area, a wing with higher aspect ratio has a longer wing span and shorter wing chord length than a wing with lower aspect ratio. Concerning civil transport aircraft, wing aspect ratio values have continuously increased. An Airbus A300 from the 1970's has an aspect ratio of approximately 7.7, while an Airbus A350 from the year 2013 has as aspect ratio of approximately 9.3. Figure 1 shows the planform of the Airbus A300-600 and the Airbus A350-900 [2].

However, a high aspect ratio wing can also have disadvantages from other aircraft design perspectives. The long wing span of the high aspect ratio wing can have an adverse effect on the wing root bending moment due to the increase in the moment arm of the applied aerodynamic forces. This can lead to an increase of the wing structural mass.

In addition, the high aspect ratio wing with its high ratio between the wing span and the wing chord length can also lead to a number of aeroelastic issues. As an example, high aspect ratio wings are relatively soft in bending and torsion when compared to conventional designs. These structural dynamic properties can lead to a reduction of the flutter speed and may finally lead to structural failure.

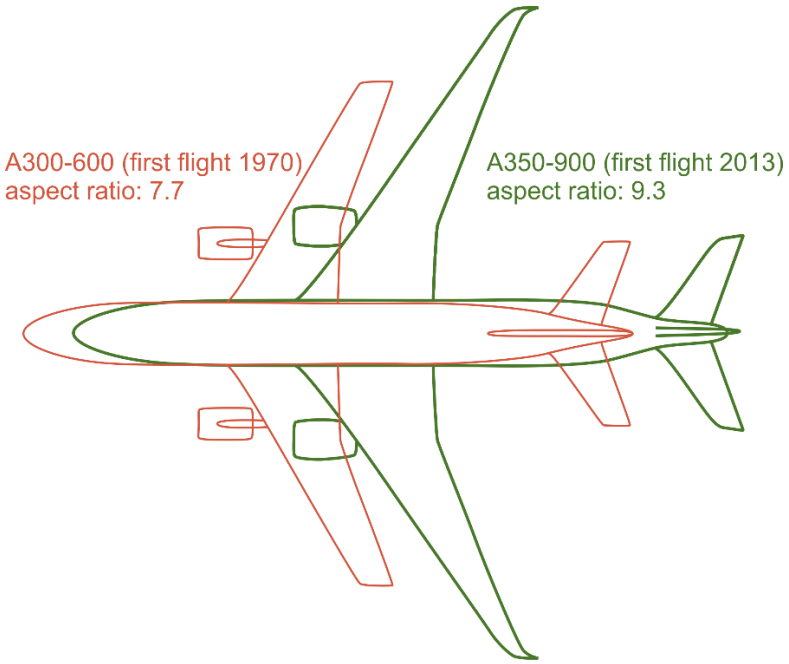

Figure 1: Comparison of the wing aspect ratio of a modern commercial aircraft with an aircraft of older design [2]

As flutter can be an important factor limiting the operational envelope of the aircraft, analyzing the flutter stability early in the design is thus important in order to avoid major design modifications at a late design phase. The German Aerospace Center, DLR, currently participates in the UP Wing (Ultra Performant Wing) project under the EU's Clean Aviation [3] funding program. The article which is presented in [2] gives an overview of the project. The initial aircraft configuration in the UP Wing project is the DLR-F25 configuration, which was originally developed in the German National Lufo VI project VirEnfREI [1]. The initial VirEnfREI configuration and the initial UP Wing configuration are nearly identical with the same wing aspect ratio of more than 15. However, they differ in wing airfoils and thus in the internal structure, eventuating in different spar heights. The DLR Institute of Aeroelasticity is responsible for the preliminary aeroelastic evaluation for both configurations. This paper will compare results of preliminary aeroelastic stability assessments and discuss influences from the wing structural design on the dynamic behavior of the wings of both configurations.

The paper begins with the description of the reference aircraft, the reference mass cases and the flight conditions. The next section describes the DLR in-house automated aeroelastic structural design and analysis tool cpacs-MONA [4] which is used for the preliminary flutter assessment. Furthermore, the simulation models are described, followed by the results of the aeroelastic assessment. The conclusion and outlook are given in the last section of the paper.

2 REFERENCE AIRCRAFT

In this work, the short/medium-range configuration DLR-F25, which is mentioned above, is taken as reference. The aircraft main characteristics are its high aspect ratio of more than 15, its body mounted main landing gear and its ultra-high bypass ratio, UHBR, engine. Table 1 lists selected key parameters of the aircraft.

Table 1: Key parameters of the DLR-F25 configuration, [1]

Parameter	**Value**
Aspect Ratio	>15
Maximum zero-fuel mass	72000 kg
Maximum landing mass	74800 kg
Maximum take-off mass	86000 kg
Cruise Mach number	Mach 0.78
Maximum operating speed, Mach number	180 m/s EAS, Mach 0.82

In this work two DLR-F25 variants are investigated. The first variant is the initial configuration of the VirEnfREI project. The second variant is the initial configuration used in the UP Wing project. Both variants have the same engine, the same engine pylon, the same engine position, the same landing gear configuration, the same wing planform, the same wing aspect ratio, the same wing twist distribution along the main wing and a comparable relative profile thickness distribution along the span, see Figure 2. The modifications are mainly driven by aerodynamic considerations, the aircraft differ in wing airfoils. It should be emphasized that, while the comparison of the aeroelastic properties presented here addresses the initial configurations, both wing designs have since been further developed in the respective projects.

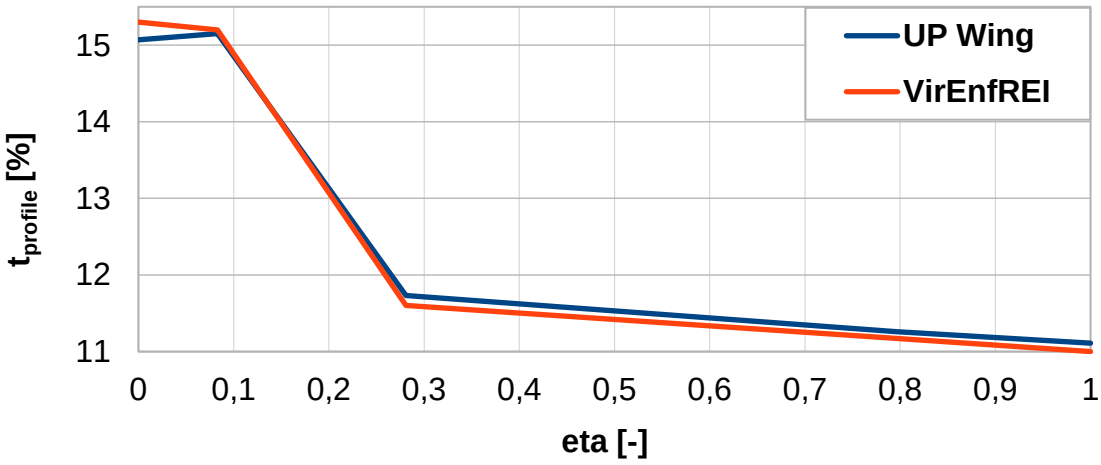

Figure 2: Relative profile thickness distribution of the two investigated configurations

2.1 Reference Mass Cases and Flight Conditions

The following section describes the reference mass cases and flight conditions for the aeroelastic stability analysis of this work.

The flutter assessment of both aircraft variants has been performed for five selected mass cases. Both aircraft have started with the same mass cases, which are, however, subject to changes as both projects proceed. These five mass cases have been used for the subsonic flutter analysis in two flight altitudes of 0 meters and 8000 meters. The density according to the international

standard atmosphere is set to 0.525 kg/m³ for a flight altitude of 8000 m and 1.225 kg/m³ at sea level. The considered Mach number is 0.6 for both altitudes. Table 2 gives an overview of the considered five mass cases, the composition of fuel (percentage of maximum fuel capacity) and payload/passenger conditions and the aircraft center of gravity positions (percentage of the mean aerodynamic chord, MAC).

Table 2: Overview of the mass cases (a combination of payload and fuel) and the aircraft center of gravity positions (percentage of the mean aerodynamic chord)

Mass Case ID	MOOee	MTAAa	MTFAa	MZAAe	MZFAe
Design Mass	OWE	MTOW	MTOW	MZFM	MZFM
Payload	0%	100%	100%	100%	100%
Fuel	0%	72%	72%	0%	0%
Aircraft CG (%MAC)	25%	40%	13%	40%	15%

3 THE CPACS-MONA PROCESS

The aeroelastic simulation models of both variants are generated and structurally optimized with the DLR-in-house parametric aeroelastic design process, cpacs-MONA. The following section gives an overview of the process.

The early considerations of aeroelastic aspects have become more and more important for the structural design of aircraft components. Together with the aerodynamic design they are a central aspect of the overall design of an aircraft. This is particularly addressed in the concurrent consideration of aerodynamic and structural design in the field of multidisciplinary optimization (MDO). Furthermore, especially for large aircraft the flexibility of the structure cannot be neglected regarding the assessment of loads, performance, maneuverability and aeroelasticity.

DLR has developed an aeroelastic structural design and analysis tool called MONA [4] which has been applied in various research projects in the recent years. The process begins with the parametric set-up of all the necessary simulation and optimization models for the aeroelastic structural design process, using the DLR in-house program ModGen, see Figure 3, top. Next, a load analysis loop is performed using MSC NASTRAN, Figure 3, bottom left. The resulting loads are used to size the structural elements defined by ModGen, Figure 3, bottom right. The sizing is performed using the structural optimization capabilities in MSC NASTRAN.

cpacs-MONA is an extension of this process. The parametric model set-up with ModGen is based on parametrically defined geometry models of the wing-like components and the fuselage. This comprises the outer geometry and all significant elements of the load carrying structure. The design process cpacs-MONA is based on MONA, but cpacs-MONA exhibits a far higher automation of the process, in order to be used as a tool in more extensive design and MDO environments [5]. Another outstanding feature of cpacs-MONA is the interfacing with a proper CPACS dataset of an aircraft configuration.

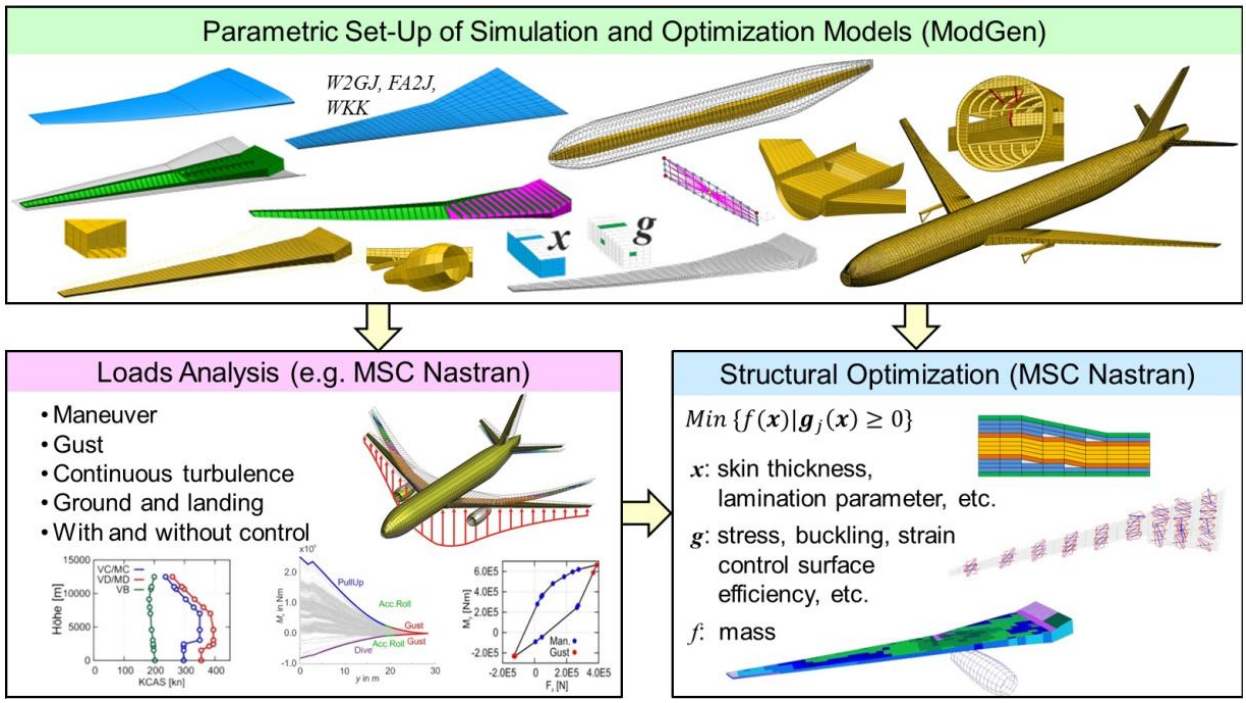

Figure 3: Basic DLR MONA process [4]

The Common Parametric Aircraft Configuration Schema (CPACS) is a data definition using XML text format for the air transportation system [6]. CPACS describes a wide range of characteristics of the aircraft, like the geometry, global aircraft parameter, the structural construction concept, material data etc., in a structured, hierarchical manner. Not only product but also process information is stored in CPACS, like aerodynamic data, aircraft loads, or mass data.

cpacs-MONA reads information from the CPACS dataset about the wing planform, the wing topology like ribs, spars and stringer initial thicknesses and positions together with the engine, pylon and landing gear positions and dimensions. It also uses information about aircraft masses like design, primary and secondary masses plus the dimensions of the control surfaces and fuel tanks.

After the extraction of the aircraft information from the CPACS dataset, a parametric finite element model is set up using the model generator ModGen, which has been described in Figure 3 above, followed by an extensive load analysis campaign of the flexible aircraft and a structural optimization of the wing structures. Finally, a subsonic flutter analysis is performed at the end of the process. Figure 4 gives an overview of the cpacs-MONA process. Detail description of the process is given in [4].

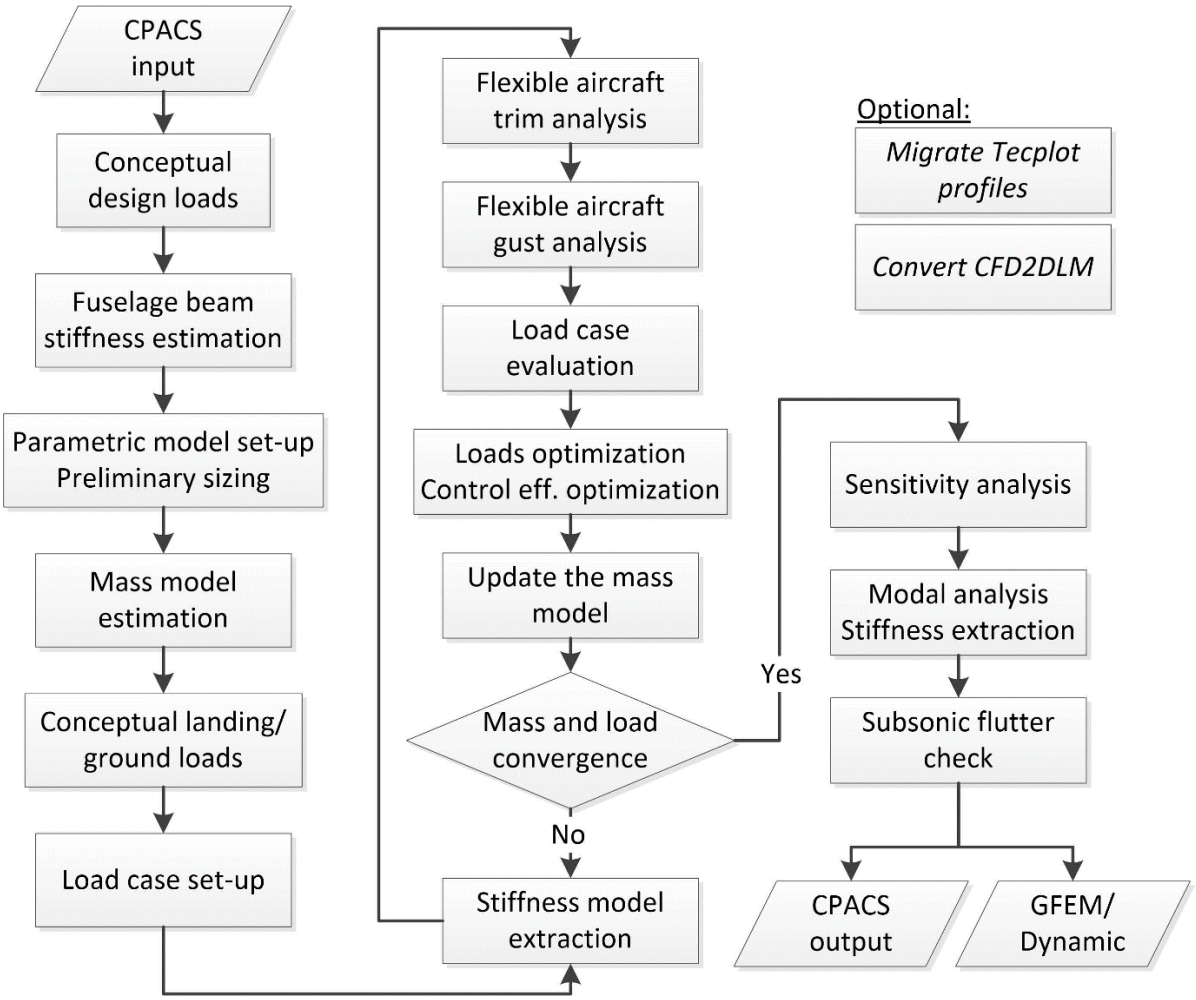

Figure 4: Process flow of cpacs-MONA [4]

4 AEROELASTIC SIMULATION MODELS

The following section describes the aeroelastic simulation models of the reference aircraft which are created by cpacs-MONA for the flutter assessment in this work. The structure of the lifting surfaces is modelled with shell elements and the fuselage is represented by beam elements. Figure 5 visualizes the MSC Nastran [7] finite element model of the DLR-F25 UP Wing. The shell elements on the fuselage and engine cowlings are for illustrational purpose only. It should be noted in this work, that as the two considered DLR-F25 variants have different wing airfoils, they have different wing section thicknesses in the chordwise direction at various wing position along the wing span. This difference is one of the causes of their differences in the structural behavior and will be discussed in Section 5.

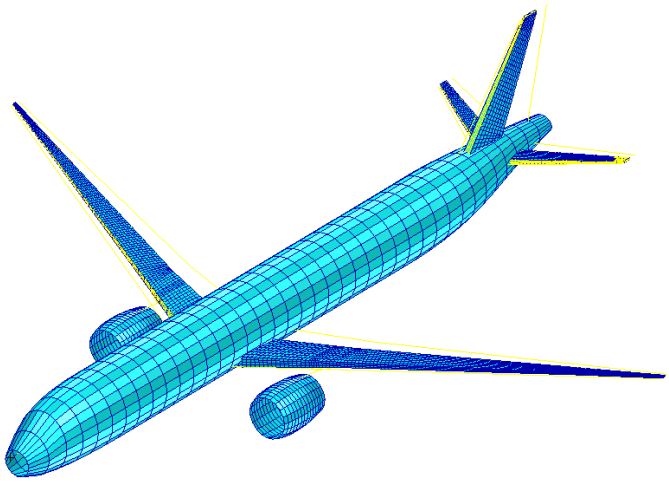

Figure 5: Global FE model of the DLR-F25 UP Wing

The aerodynamic forces are modelled using the potential theory, namely the vortex lattice method (VLM), for the quasi-steady cases and doublet lattice method (DLM), for the dynamic cases within MSC NASTRAN. Moreover, a slender body element and a corresponding set of interfering lifting surfaces are created to take the aerodynamic effect of the fuselage into account. For the lifting surfaces, a twist and camber correction is considered, which evoke non-zero lift and pitch moment at zero angle of attack. Figure 6 shows, as an example, the aerodynamic model of the DLR-F25 UP Wing including the slender body for its fuselage.

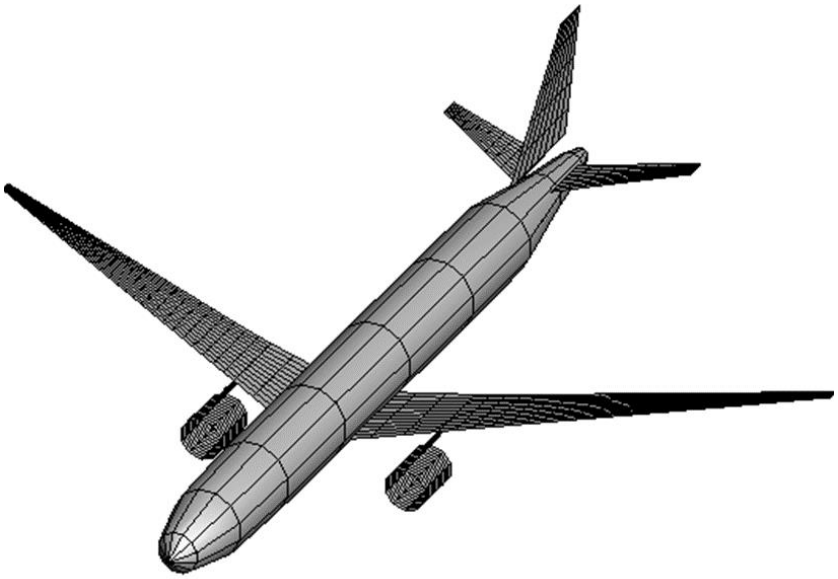

Figure 6: Aerodynamic model of the DLR-F25 UP Wing

Using the above simulation model, a flutter calculation using MSC NASTRAN Solution 145 [8] is performed at the end of the cpacs-MONA process for both aircraft variants. The non-matched flutter analysis is employed, using the p-k-Method with fixed Mach number and fixed density.

5 RESULTS

In this work, the major goal is to compare the result from both configurations in order to illustrate the effects of the difference in the wing structural design to the aircraft aeroelastic behavior rather than to publish the exact value of the result.

5.1 Wing structural elasticity

As mentioned previously, both considered DLR-F25 variants differ in their wing airfoils. Both wings share the same leading and trailing edge lines along the span, leading to the same twist distribution. Although the relative profile thickness along the span is nearly identical, the chordwise thickness distribution varies, see Figure 7a. This results in different internal structures of the wings, visible for example in the height of the spars. Figure 7b shows the different spar heights of these two aircraft over the relative spanwise coordinate eta. Due to the different airfoils, the front spar of the UP Wing configuration is higher in the inner wing and slightly lower in the outer wing than the initial VirEnfREI configuration, while the rear spar is up to 17% higher along the full wing span. This difference, among others, has an influence on global wing structural stiffness.

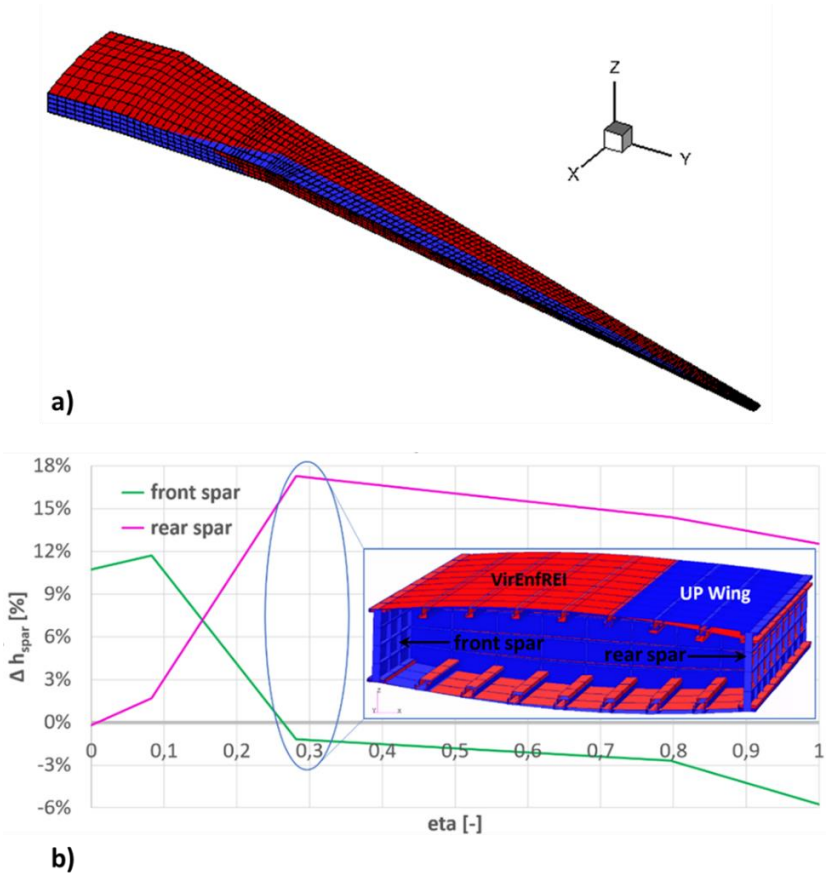

Figure 7: a) The finite element models of the right main wing of the UP Wing configuration (blue) and the VirEnfREI configuration (red) b) Relative spanwise spar heights of the UP Wing wing (blue) in comparison to the VirEnfREI wing (red)

Table 3 compares the major structural elasticity properties of the two DLR-F25 variants which are a result of the different spar heights. It shall be noted that in the Table the values from the

VirEnfREI variant are taken as reference (100%). Figure 8 shows, as an example, the first symmetric wing bending mode and the first symmetric wing torsion mode for the MOOee mass case of the DLR-F25 UP Wing variants.

Table 3: Comparison of major structural elasticity properties of the DLR-F25 UP Wing configuration in comparison to the VirEnfREI configuration for the MOOee mass case

	Deviation
1st symmetric wing out-of-plane bending eigenfrequency	+0.5%
1st symmetric wing torsional eigenfrequency	+3%
Vertical tip displacement at 1g cruise condition	-11%

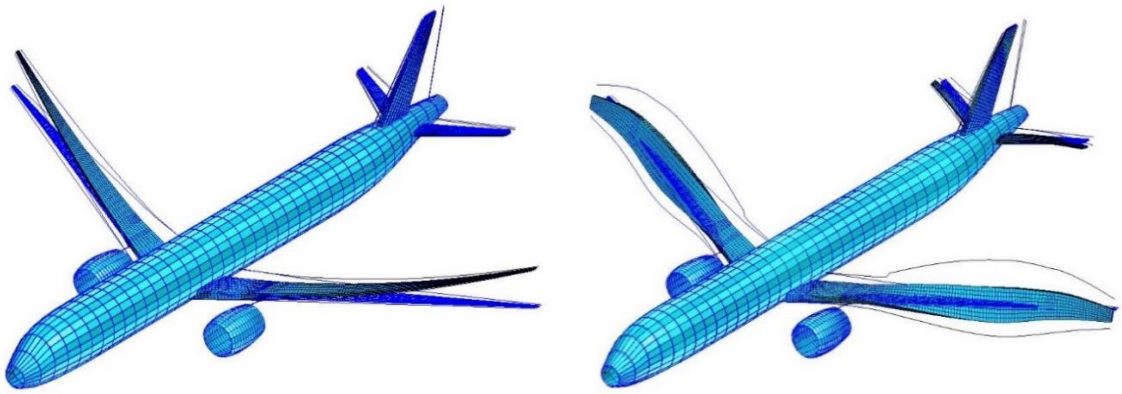

Figure 8: 1st symmetric wing bending mode (left) and the 1st symmetric wing torsion mode (right) for the MOOee mass case of the DLR-F25 UP Wing variant

The first symmetric wing bending eigenfrequencies of both configurations are similar. However, concerning the first symmetric wing torsion mode, the VirEnfREI variant has a slightly lower eigenfrequency than the UP Wing variant. In the case of the wing tip deflections at cruise condition, the UP Wing variant has distinctly less wing tip vertical deflection (translation in z-direction) compared to the VirEnfREI configuration. Values in the Table 3 indicate that the VirEnfREI wing is softer than the UP Wing wing.

5.2 Flutter analysis

The objective of this work is not to present the exact value of the result such as the flight envelope boundary velocities and the flutter velocities of both aircraft. The objective of this work is a comparison of the effect of the relevant structural properties on the aircraft aeroelastic characteristics, especially to assess the flutter characteristics of both configurations. This understanding is valuable during the early preliminary design phase.

One example will be given for the MOOee mass case. Here, the flutter velocity of the UP Wing configuration is higher compared to that of the VirEnfREI aircraft. One of the possible reasons for the higher flutter speed of the UP Wing configuration is the difference of their internal main wing structures as discussed above. The higher rear spar results in a stiffer wing for the UP Wing configuration. Consequently, the torsion and bending eigenmodes of the softer VirEnfREI wing

couple at a lower speed with the engine pitching eigenmode, thus resulting in a lower flutter velocity of the VirEnfREI configuration. The dominant structural eigenforms for both configurations are the engine pitch mode, coupling with the eigenmodes of wing bending, wing torsion and fuselage bending. Figure 9 illustrates this eigenmode.

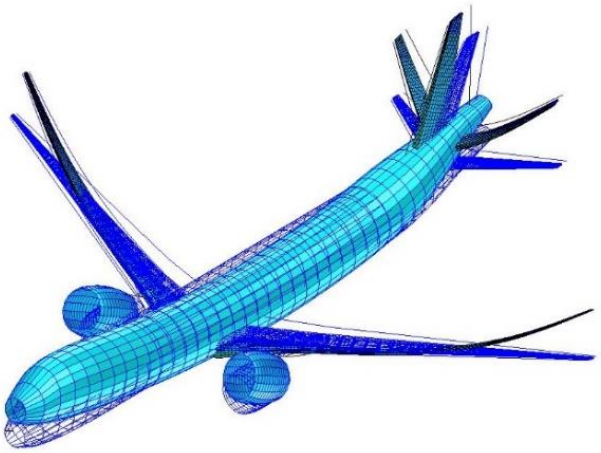

Figure 9: The 5th elastic eigenmode of the FEM of the DLR-F25 UP Wing configuration.

A strong influence of the engine/pylon modes coupling with the wing modes has been experienced in previous research work, see e.g. [9], where the aeroelastic behavior of the wing of a long-range aircraft with a UHBR engine is investigated. One of the causes of this coupling is the stiffness of the engine pylon. The sizing of the pylon is first of all defined by strength constraints subject to static and dynamic accelerations, i.e. the pylon has, of course, to be strong enough to support the engine mass. Second, at flight speed, the engine has to withstand aerodynamic forces and must not diverge. The geometric layout of the pylon and the sizing of the structure yields the structural stiffness which strongly influences the wing modes. However, as there are a large number of possible design variables in a pylon design, the resulting structural stiffness at a preliminary design stage is still subject to a large uncertainty.

Figure 10 visualizes the parametrized structural model of the pylon for a wing mounted engine as it is realized within ModGen. The finite element model represents a generic, simplified design, with the parameters chosen according to experience with existing aircraft. More details on the parametric modeling for the wing integration of the engine and pylon within cpacs-MONA are described in [10].

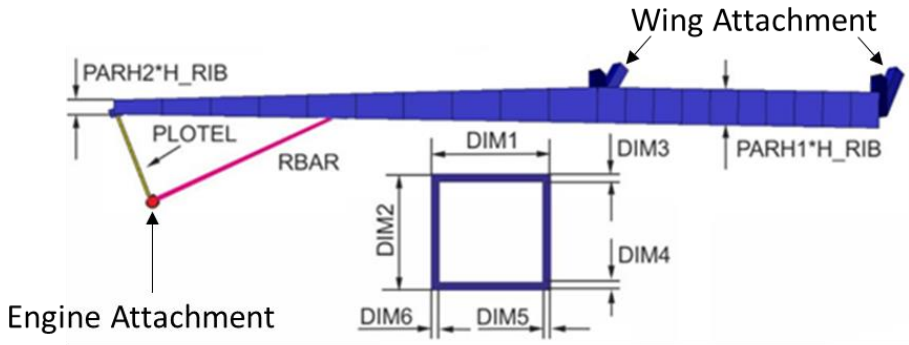

Figure 10: Visualization of the parameters for the structural pylon modelling in ModGen, [9]

In [9], the two parameters defining the beam height at the front and rear of the pylon beam (PARH1 and PARH2) were increased with respect to the initial design in order to shift the eigenfrequencies of the engine modes to higher frequencies. The stiffer pylon successfully shifted the flutter velocity to a higher flight speed.

In this work, the beam height has at first also been increased to stiffen the pylon. However, this has not led to the desired effect. The flutter velocity even decreased when the pylon stiffness increased. Instead, the values for the parameters PARH1 and PARH2 had to be decreased in order to decouple the engine eigenmode from the wing eigenmode. Figure 11 illustrates, as a result example, the flutter curves of the UP Wing configuration for the MOOee mass case at the flight altitude of h = 8,000 m for the Mach number Ma = 0.6 with the initial engine pylon parameters and with the decreased parameters. The flutter analysis is performed using the first 56 eigenmodes including the six rigid-body-modes. For a better visualization, only the most relevant elastic modes up to mode number 36 are plotted. Modes in light grey have a monotonically falling damping value within the aeroelastic stability envelope and no significant change in frequency. As shown in Figure 11, with the decreased pylon parameters the flutter velocity is shifted to higher flight speeds outside the aeroelastic stability envelope (1.15*VD). On the left side, Mode 11 (5th elastic mode as highlighted in Figure 9) shows a positive damping within the aeroelastic stability envelope, while at the right diagram, Mode 11 is detected to be non-critical. The required parameter changes were inside the strength requirements.

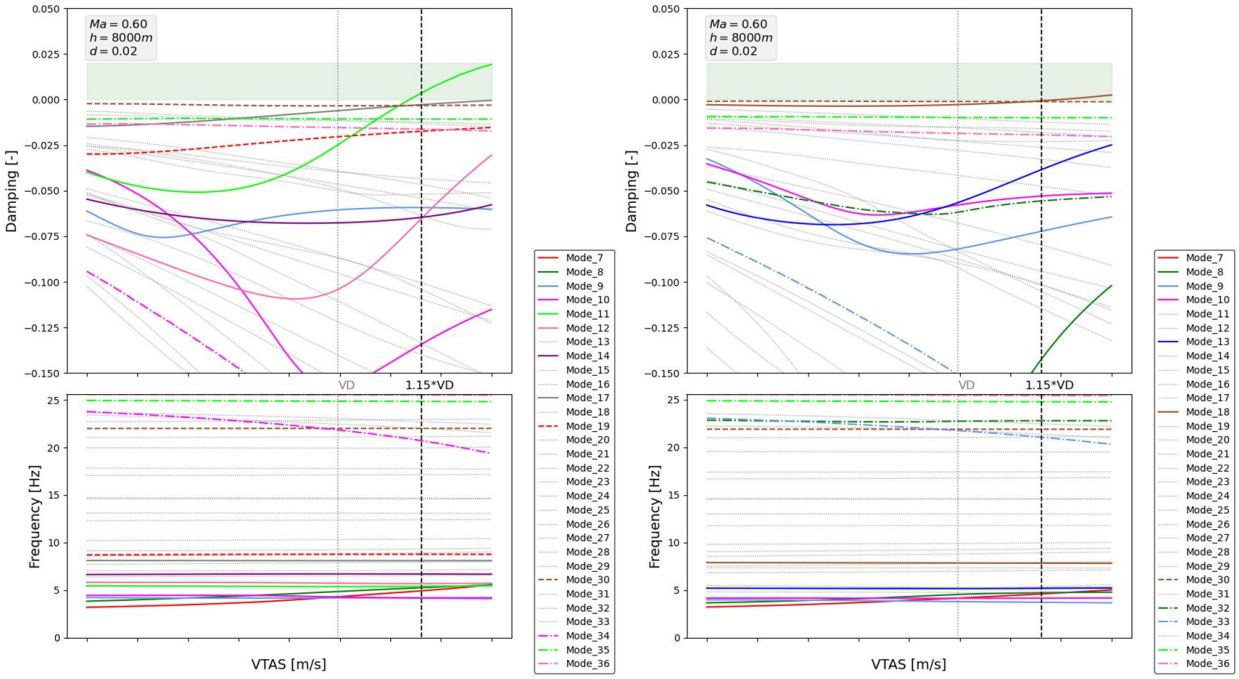

Figure 11: Flutter curves of the UP Wing configuration for the MOOee mass case at the h = 8,000 m for the Ma = 0.6 with the initial engine pylon parameters (left) and the decreased pylon beam height (right)

6 CONCLUSIONS AND OUTLOOK

This work has demonstrated the aeroelastic structural preliminary design and analysis processes of two variants of the DLR-F25 high aspect ratio civil transport aircraft. The DLR parametric design process cpacs-MONA has been used to analyze and evaluate the aeroelastic stability behavior of the aircraft. The results show that even though both aircraft are nearly identical, a moderate change in the airfoil thickness distribution along the chord, due to aerodynamic optimization, can lead to a significant change in the structural dynamics, i.e. the eigenfrequencies and -modes, and thus in the resulting flutter speed.

The analyses also demonstrate the significant influence of the pylon stiffness on the coupling of the elastic engine/pylon eigenmode with the wing eigenmodes, and thus on the flutter characteristics. By adapting parameters of the elastic pylon model within cpacs-MONA, the flutter velocities could be shifted to higher airspeeds. This awareness on the effect of the engine/pylon eigenmode early during the preliminary design step can prevent major design modifications later in the detail design phase.

At the status of this publication, both the VirEnfREI and the UP Wing projects are ongoing activities. Further evaluations of the aeroelastic stability of the configurations under development will be performed later in the projects, and the final aeroelastic characteristics of both aircraft can only be evaluated at the last design phase, when the designs are frozen and all the required information are available. Additionally, the engine/pylon modelling in ModGen is currently extended.

ACKNOWLEDGMENTS

The project VirEnfREI is funded by

on the basis of a decision of the Deutsche Bundestag.

The project UP Wing is funded by the Clean Aviation Joint Undertaking (JU) under the Grant No. 101101974, financed by the Research and Innovation Program Horizon Europe of the European Union.

REFERENCES

[1] https://www.dlr.de/de/as/forschung-transfer/projekte/virenfrei (Accessed 25 April 2024)

[2] https://www.dlr.de/en/ae/latest/news/new-wing-concepts-for-transport-aircraft-less-co2-through-higher-aspect-ratios (Accessed 22 April 2024)

[3] https://www.clean-aviation.eu (Accessed 01 April 2024)

[4] T. Klimmek, M. Schulze, M. Abu-Zurayk, C. Ilic, A. Merle, "cpacs-MONA – An independent and in high fidelity based MDO tasks integrated process for the structural and aeroelastic design for aircraft configurations," in: International Forum on Aeroelasticity and Structural Dynamics 2019, IFASD 2019, Savannah, GA (USA).

[5] R. Liepelt, V. Handojo, and T. Klimmek, "Aeroelastic analysis modelling process to predict the critical loads in an MDO environment," in: IFASD International Forum on Aeroelasticity and Structural Dynamics, 28 June - 2 July, 2015, Saint Petersburg (Russia)

[6] B. Nagel, D. Böhnke, V. Gollnick, P. Schmollgruber, A. Rizzi, and G. La Rocca J.J. Alonso, "Communication in aircraft design: Can we establish a common language?," in: ICAS, 28th International Congress of the Aeronautical Sciences, 23-28 September 2012, Brisbane (Australia)

[7] MSC Corporation, "MSC Nastran 2018.2 - Aeroelastic Analysis User's Guide," 2018.

[8] MSC Software Corporation, MSC Nastran 2021 Aeroelastic Analysis User's Guide, United States of America: HEXAGON, 27. Nov. 2020.

[9] M. Schulze, T. Klimmek, F. Torrigiani and T. F. Wunderlich, "Aeroelastic Design of the oLAF Reference Aircraft Configuration," in: Deutscher Luft- und Raumfahrtkongress (DLRK) 2021, 31 August – 2 September 2021, Bremen, Germany (virtual)

[10] M. Schulze, J. Neumann, and T. Klimmek, "Parametric Modeling of a Long-Range Aircraft under Consideration of Engine-Wing Integration," in: Aerospace, 8 (1), pp. 1-20. Multidisciplinary Digital Publishing Institute (MDPI). ISSN 2226-4310, 2021.

COPYRIGHT STATEMENT